Rheol Acta 36:429–448 (1997)

ORIGINAL CONTRIBUTION

Can extensional viscosity be measured with opposed-nozzle devices?

Prasannarao Dontula
Matteo Pasquali
L.E. Scriven
Christopher W. Macosko

Received: 7 October 1996
Accepted: 13 February 1997

Dedicated to the memory
of Anastasios C. Papanastasiou

P. Dontula · M. Pasquali · L.E. Scriven
Prof. Dr. Ch.W. Macosko (✉)
Department of Chemical Engineering
& Materials Science
University of Minnesota
421 Washington Avenue S.E.
Minneapolis, Minnesota 55455, USA

Abstract Opposed-nozzle devices are widely used to try to measure the extensional viscosity of low-viscosity liquids. A thorough literature survey shows that there are still several unanswered questions on the relationship between the quantity measured in opposed-nozzle devices and the "true" extensional viscosity of the liquids. In addition to extensional stresses, opposed nozzle measurements are influenced by dynamic pressure, shear on the nozzles, and liquid inertia. Therefore the ratio of the apparent extensional viscosity that is measured to the shear viscosity that is independently measured is greater than three even for Newtonian liquids. The effect of inertia on the extensional measurements is analyzed by computer-aided solution of the Navier-Stokes system, and by experiments on low-viscosity Newtonian liquids (1 mPa s$\leq\eta_S\leq$800 mPa s). The effect of nozzle separation-to-diameter ratio on the average residence time of the liquid is analyzed under the assumption of simple extensional flow kinematics. The average residence time of the liquid is independent of this ratio unless the radial inflow section of the extensional flow volume is related to the nozzle separation. Experiments indicate that in some cases widening the gap lowers the apparent extensional viscosity that is measured, whereas in other cases the opposite is true. In the light of these theoretical considerations and experimental observations, the use of systematic corrections to extensional viscosity measurements on non-Newtonian liquids is not recommended. Thus opposed nozzle devices should be considered as useful indexers rather than rheometers. Finally, measurements on a series of semi-dilute solutions of high molecular weight poly(ethylene oxide) in water are also reported.

Key words Extensional viscosity – extensional flow – elongational viscosity – opposed nozzles – extensional rheometry

Introduction

Frequent applications in coating and polymer processing employ liquids that show substantial to dramatic deviations from Newtonian behavior. Process liquids are subjected to large strains and very intense strain rates in the complex deformation and flow fields occurring in the apparatus. Shear measurements are not sufficient to completely characterize the rheological behavior of the liquid in such cases and must be supplemented by measurements obtained in extension or extension-like deformations.

Extensional flow fields cannot be generated easily (Winter et al., 1979; Macosko, 1994). Low viscosity liquids cannot be gripped between rotating clamps and hence techniques used for solid-like materials (approximately $\eta_S\geq10^3$ Pa s) are not suitable for these liquids. Fiber-spinning and filament stretching are the best tech-

niques to approximate extensional flows of intermediate viscosity liquids (approximately 10^3 Pa s$\geq\eta_S\geq$10 Pa s). However, many low-viscosity liquids like polymer solutions, gelatins, inks, low concentration suspensions, etc. cannot be drawn into fibers, and therefore cannot be tested by fiber-spinning (Secor et al., 1989).

Winter et al. (1979) suggested orthogonal stagnation flows to measure properties of polymeric liquids in steady extension, and discussed the applicability of several methods to generate such flows. Lubricated die flows have been used to measure extensional viscosity of high viscosity liquids in biaxial extension (van Aken and Janeschitz-Kriegl, 1980), and in planar extension (Macosko et al., 1982). However, the roughly double stagnation flow between opposed nozzles is perhaps the best technique presently available to characterize the extensional response of low viscosity liquids (roughly $\eta_S\leq$10 Pa s). The opposed-nozzle device used in this study is the Rheometrics RFX Fluid Analyzer, the commercial version of the instrument proposed by Fuller et al. (1987). A schematic of the apparatus is depicted in Fig. 1. During the test, liquid is drawn into two opposed nozzles mounted on rigid arms by the action of two syringes driven by a stepper motor. The right nozzle arm is fixed, whereas the left arm can rotate about a pivot. When liquid is drawn into the nozzles, a torque M must be applied to the pivot to balance the force induced by the flowing liquid on the nozzle and prevent movement of the left arm. The force $f_R \equiv \frac{M}{L}$ needed to balance the hydrodynamic force on the nozzles is related to what is defined as the liquid's effective extensional viscosity η_E:

$$\eta_E \equiv \frac{1}{\dot{\varepsilon}}\frac{f_R}{\pi R^2} = \frac{M}{\dot{\varepsilon}\pi R^2 L} \,. \tag{1}$$

Here R is the radius of the nozzles and L is the distance between the pivot and the symmetry axis through the nozzles. The apparent extension rate in the flow $\dot{\varepsilon}$ is defined in terms of the liquid flow rate Q into one nozzle and the gap $2h$ between the nozzles by

$$\dot{\varepsilon} \equiv \frac{Q}{\pi R^2 h} \,. \tag{2}$$

In some works on opposed-nozzle rheometry (Chow et al., 1988), Q is defined as the *total* flow rate into *both* nozzles; h, or sometimes d, is often defined as the *total* separation between the nozzles. Contradicting definitions are sometimes found within the same work (Hermansky and Boger, 1995). Therefore it is advisable to check a paper's definition(s) to avoid possible confusion.

Equation (2) follows from the hypothesis of steady homogeneous uniaxial extensional flow between the nozzles, viz.

$$\boldsymbol{v} = \dot{\varepsilon} z \boldsymbol{e}_z - \dot{\varepsilon}\frac{r}{2}\boldsymbol{e}_r \tag{3}$$

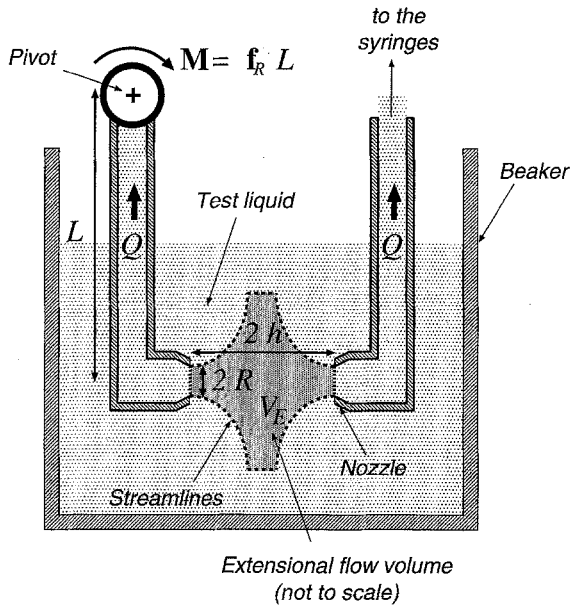

Fig. 1 Schematic of the RFX opposed-nozzle device. The putative extensional flow volume is shaded and not drawn to scale

z and r being the axial and radial coordinates, whose origin is fixed at the stagnation point.

As shown by Schunk et al. (1990) and Pasquali and Scriven (1996), this kinematic hypothesis is not sufficient to ensure that the only force acting on the nozzle is the difference between axial and radial normal stresses which underlies Eq. (1). Several additional, and rather arbitrary, approximations and assumptions are required to arrive at Eq. (1). Therefore, Eq. (1) should be considered a *definition* of an apparent opposed-nozzle extensional viscosity, rather than the result of a force balance on the nozzles.

This measured extensional viscosity does not coincide in general with the extensional viscosity η_U which is defined as ratio of the difference between axial and radial stresses, $\tau_{zz} - \tau_{rr}$, to axial rate of extension, $\dot{\varepsilon}$,

$$\eta_U \equiv \frac{\tau_{zz} - \tau_{rr}}{\dot{\varepsilon}} \,. \tag{4}$$

Therefore the ratio of extensional viscosity measured in the opposed-nozzle device to shear viscosity η_E/η_S, sometimes inappropriately referred to as Trouton ratio, is not equal to 3 even in Newtonian liquids, as discussed by Schunk et al. (1990, p. 401). In the following, the ratio of measured apparent extensional viscosity to shear viscosity is denoted by $T_A \equiv \frac{\eta_E}{\eta_S}$.

Literature review

Double stagnation flows have been frequently used in the past to approximate extensional flow kinematics.

The idea was first pursued by Taylor (1934) in the four-roll mill. Double stagnation flows generated by sucking (or blowing) liquid into opposed nozzles have been used in the last two decades to approximate uniaxial extensional flow (or biaxial compressional flow in some cases). Frank et al. (1971) first studied chain extension and flow-induced crystallization with this technique. Later, in an extensive study, Mackley and Keller (1975) examined flow-induced crystallization of polyethylene melts in such a geometry. Using flow visualization as well as birefringence, they found that the flow generated between two aligned opposed nozzles is predominantly extensional in nature, but some shear is still present. Pope and Keller (1978) studied the effect of flow between opposed nozzles on molecular orientation with polystyrene solutions.

Viscosity measurements were first attempted by two different groups with two different methods. Keller et al. (1987) and Chow et al. (1988) tried to estimate an effective extensional viscosity in opposed-nozzle flow by measuring the pressure drop across the nozzles. Neither work reports a quantitative analysis of the dependence of the measured pressure drop on extensional viscosity and on other flow quantities.

At the same time, Fuller et al. (1987) proposed an alternative method to measure extensional viscosity based on a *force* measurement rather than *pressure drop* in opposed-nozzle flow. They were the first to relate *quantitatively* an apparent extensional viscosity to measurable dynamic quantities in the opposed-nozzle configuration. They measured the force needed to balance the hydrodynamic force exerted by the flowing liquid on one of the nozzles, and related it to the liquid's apparent extensional viscosity η_E through Eq. (1). The apparent extension rate in the flow $\dot{\varepsilon}$ was related to the flow rate Q into one nozzle through Eq. (2). Fuller et al. measured the extensional viscosity of Newtonian glycerin-water solutions and found that it was 2.25 to 3.6 times the shear viscosity of the solutions over extension rates $\dot{\varepsilon}$ ranging from 400 to about 4000 s^{-1}. They also applied the technique to xanthan solutions and polyacrylamide solutions in glycerin/water and found that the effective extensional viscosity of the polyacrylamide solutions grew with extension rate, whereas that of xanthan solutions changed scarcely at all with extension rate.

Mikkelsen et al. (1988) perfected the design of Fuller et al. (1987). Their experiments on Newtonian liquids confirmed that a nozzle gap to diameter ratio $\frac{2h}{2R} = 1$ is optimal. They found that measurements of extensional viscosity made with sharp nozzle angles and sharp edges were closer to thrice the shear viscosity of the liquid in the range of extension rates where inertia was not important. Measurements on low-viscosity glycerin/water solutions showed that, in extension, the measured extensional viscosity rises with extension rate at Reynolds number $\mathrm{Re} \approx 20$, whereas in compression the rise begins earlier, at $\mathrm{Re} \approx 5$. Mikkelsen et al. attributed the increase in *both cases* to inertia.

Opposed-nozzle flow was successfully used by Cathey and Fuller (1988) to characterize extensional properties of solutions of collagen in glycerin and water at various concentration over a range of apparent extension rates $\dot{\varepsilon} \approx 10$–$650\ s^{-1}$. Lower concentration solutions showed rate-independent apparent extensional viscosity; the more concentrated ones displayed extension-thinning behavior.

Succeeding studies by Cathey and Fuller (1990) focused on both optical and mechanical measurements on the flow of dilute solutions of flexible polymers. Optical birefringence measurements showed that the retardation angle was maximum near the stagnation point and fell rapidly as the polarized light beam was moved away from it. The measured retardation profiles became unsteady at high extension rates with high molecular weight solutions. According to Cathey and Fuller, this flow instability was related to the onset of intermolecular interactions such as entanglements. Cathey and Fuller also speculated on the effect of the average total strain experienced by the molecules and on the effect of the average residence time in the flow field. They estimated the average strain $\bar{\varepsilon}$ and residence time $\bar{t}_R$ by averaging the strain and residence time of fluid elements over a nozzle face, and they reported $\bar{\varepsilon} \approx 1$ and $\bar{t}_R \approx \dot{\varepsilon}^{-1}$.

Schunk et al. (1990) confirmed the experimental results of Mackley and Keller (1975) regarding the mixed nature of the flow field between opposed nozzles. They examined the flow of a Newtonian liquid around a nozzle by solving the Navier-Stokes equation system with Galerkin's method of weighted residuals and finite element basis functions. Plots of the Giesekus function (Fig. 4 of their paper) show that pure extension is achieved only in proximity of the stagnation plane between the nozzles and near the nozzle's symmetry axis; elsewhere shear (rotation) coexists with extension in large regions. The same qualitative results were obtained in a later work by Schunk and Scriven (1990, Fig. 4) by using a frame-indifferent reformulation of Giesekus' flow criterion.

Schweizer et al. (1990) used a prototype Rheometrics RFX opposed-nozzle device to study the extensional behavior of the test fluid M1. A wide range of extension rates was achieved by using nozzles of different diameter. They reported that the apparent Trouton ratio T_A, that is the ratio of the low-rate apparent extensional viscosity to the zero-shear viscosity of M1, was $T_A \approx 4.2$. Schweizer and coworkers also found that the apparent extensional viscosity of M1 was independent of nozzle separation at low extension rates ($\dot{\varepsilon} \leq 1\ s^{-1}$), and that it rose with nozzle separation at higher rates. This rise in extensional viscosity at large gaps was at-

tributed to longer average residence times in the flow and therefore higher total strains on the polymer molecules.

Laun and Hingmann (1990) also used an opposed-nozzle device to estimate the extensional viscosity of fluid M1. They achieved only a limited range of extension rates ($\dot{\varepsilon} \approx 20$–$60\ s^{-1}$) and reported apparent extensional thickening behavior of fluid M1. The measurements of apparent extensional viscosity reported by Laun and Hingmann are in good agreement with those of Schweizer et al. (1990). Laun and Hingmann also reported measurement on pure glycerin and solutions of glycerin and water. They report apparent Trouton ratios in the range $T_A \approx 3-5$. The apparent Trouton ratio grew once the extension rate exceeded a critical value that depended on the solution viscosity. The onset of the growth in ratio T_A occurred at a higher extension rate the lower the viscosity of a solution.

Cai et al. (1992) compared several extensional rheometers with low-viscosity liquids. They reported that the ratio of measured apparent extensional viscosity in opposed nozzles to shear viscosity of a solution of glycerin and water ($\eta_S = 27$ mPa s) ranged between 4 and 5 over a range of apparent extension rates $\dot{\varepsilon}$ from 5 to $3000\ s^{-1}$. Lower rates were inaccessible because the transducer lacked sensitivity. Measurements at higher rates showed an increasing apparent extensional viscosity, which was attributed to inertia, as by Mikkelsen et al. (1988). Cai et al. also reported that opposed-nozzle measurements of extensional viscosity of 0.1% wt. xanthan solutions in water agreed with measurements obtained in entry flow, but that no agreement was found between measurements taken on 0.5% wt. polyacrylamide in 50/50 glycein-water mixture with fiber spinning, tubeless siphon, opposed nozzles and entry flow.

Willenbacher and Hingmann (1994) measurud the apparent extensional viscosity of test fluid S1 in the same device used by Laun and Hingmann (1990). They found a pronounced extension-thickening behavior of S1. They reported that the apparent extensional viscosity was not sensitive to nozzle radius but varied strongly with nozzle separation. Like Schweizer et al. (1990), they attributed this phenomenon to the higher average strain imposed on liquid elements at higher nozzle separation and tried to superpose apparent viscosity curves empirically, by plotting the ratio of measured extensional viscosity to nozzle separation against the product of apparent rate of strain and nozzle separation.

Anklam et al. (1994) used a commercial opposed-nozzle device, the Rheometrics RFX Analyzer, to study the behavior of water-in-oil emulsions in extensional flow. They suggested that the force measurement be corrected to account for liquid inertia; the correction they put forward to correct the viscosity measurement is (Eq. (8) of their paper):

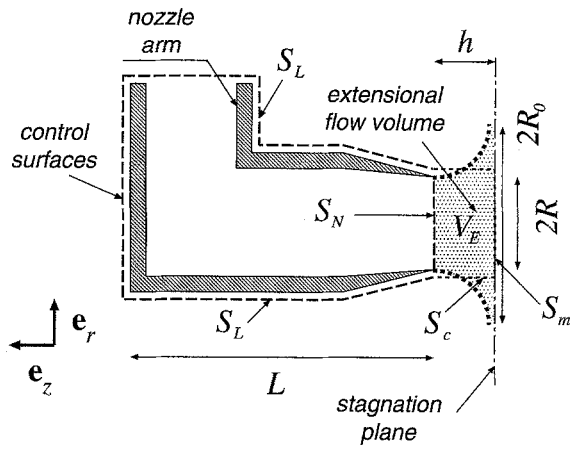

Fig. 2 Schematic of a nozzle. The extensional flow volume V_E is shaded. The control surfaces on which the momentum balances are performed are dashed. Pasquali and Scriven (1996) used $S_L + S_N$, Schunk et al. (1990) used $S_L + S_c + S_m$. The origin of the coordinate system is fixed at the stagnation point

$$\eta_{\text{corrected}} = \eta_{\text{apparent}} - \frac{\rho d^2 \dot{\varepsilon}}{8} \tag{5}$$

They derived this expression from a momentum balance on a cylindrical control surface connecting the nozzles in the extensional flow (see Schunk et al., 1990, Fig. 2 and also surface S_c in Fig. 2 of this article). The velocity on the control surface was estimated by assuming simple extensional flow, i.e. Eq. (4). Equation (5) states that liquid inertia *increases* the apparent viscosity. Anklam et al. (p. 809) also noticed that a momentum balance at the nozzle face (surface S_N in Fig. 2) would lead to an inertia correction whose value is twice that in Eq. (5). They speculated that the assumption of simple extensional flow kinematics is less certain at the nozzle's face than on the lateral cylindrical surface between the nozzles and recommended Eq. (5) for inertia corrections.

Hu et al. (1994) studied the extensional behavior of surfactant solutions with a Rheometrics RFX fluid analyzer. The ratio of their measured apparent extensional viscosity to shear viscosity with solutions of glycerin and water was approximately 3 to 3.5 over a range of extension rates $\dot{\varepsilon}$ from 5 to $1000\ s^{-1}$. They observed a slight rise in measured viscosity at high rates ($\dot{\varepsilon} \geq 300\ s^{-1}$) and attributed this effect to the "kinetic energy" of the liquid.

Hermansky and Boger (1995) studied extensional behavior of low-viscosity Newtonian and non-Newtonian liquids with a RFX. They observed that the apparent extensional viscosity of low viscosity liquids ($\eta_S \approx 1$–75 mPa s) rose strongly with apparent extension rate at rates in the range $\dot{\varepsilon}$ from 1000 to $20000\ s^{-1}$ (Reynolds number $\mathrm{Re} \approx 5$–5000). They stated that liquid inertia increased the torque at high strain rates and low viscosities, and proposed the following empirical correction to the measured torque (Eq. (2) of their paper):

$$M_{\text{measured}} = M_{\text{corrected}} + a'(R)\rho U^2 \quad (6)$$

where M_{measured} is the measured torque, $M_{\text{corrected}}$ is the "corrected" torque, i.e. the torque induced by extensional stresses, $a'(R)$ is an empirical function of the nozzle radius R, ρ is the density of the liquid and U is the average velocity of the liquid (ratio of flow rate to nozzle area). Equation (6) also states that liquid inertia *increases* the measured torque. Hermansky and Boger were seemingly able to correct the measured torque of a number of Newtonian liquids by using Eq. (6), even though this correction amounted up to 98% of the measured torques. They then used the Newtonian corrections to adjust the measured viscosities of dilute solutions of polyethylene glycol in water.

Mackay et al. (1995) recently proposed a new opposed-nozzle rheometer in which an apparent extensional viscosity is evaluated from a measurement of pressure drop between the chamber of the rheometer and the exit section of the jet, similar to that proposed by Keller et al. (1987) and Chow et al. (1988). The apparatus can be completely pressurized and heated, thereby allowing high viscosity liquids and polymer melts to be tested.

Padmanabhan (1995) recently surveyed the techniques developed to test the extensional viscosity of polymeric liquids and their applicability to food rheology. He evaluated experiments with dilute solutions of xanthan in water by Clark (1991) and suggested that opposed-nozzle devices could be successfully employed to study the extensional behavior of low-viscosity foods.

Pasquali and Scriven (1996) re-examined the working equation of the opposed-nozzle device by means of balances of momentum and mechanical energy, using the simplifying assumption of uniaxial extensional flow between the nozzles. They showed that the measured torque is affected by several contributions other than the axial viscous stresses. A balance of momentum around the nozzle reveals that the dynamic pressure at the nozzle face contributes significantly to the measured stress. This agrees with the analysis of Schunk et al. (1990). Pasquali and Scriven concluded that inertia *lowers* the measured torque, and that the shear stresses on the nozzle walls may *lower* or *raise* the measured torque, depending on whether or not a toroidal recirculation develops around the nozzles. This results is consistent with the findings of Schunk et al. (1990, Fig. 8). Two other effects may increase the measured torque at high flow rates: the extensional flow volume may become larger at high flow rates, and more and more liquid may be involved in the flow outside the extensional flow volume. The greater amount of flowing liquid causes larger viscous dissipation in the whole flow volume, and therefore makes the pressure at the front of the nozzle lower than that at the back, where the liquid is stationary. This pressure difference acts in the same direction as the liquid's tensile normal stresses and thus raises the measured torque.

Walker et al. (1996) used a RFX to measure the elongational properties of semi-dilute CPCl/Sal micellar solutions in concentrated brine. They found that the apparent extensional viscosity of these solutions rose with extension rate up to a maximum, and then fell. The maximum in apparent extensional viscosity was observed at $\dot{\varepsilon}\lambda \approx 0.7$ (λ being the material's relaxation time) at all values of concentration and temperature, and was attributed to slipping and breaking of aligned micelles at entanglement points.

Table 1 summarizes reported measurements of extensional viscosity of Newtonian liquids with opposed-nozzle devices. The values of apparent extensional viscosity and apparent Trouton ratio were read from graphs reported in the quoted studies. Usually one of these quantities was reported; the other was calculated from knowledge of the shear viscosity.

This work reconciles apparent differences found in the literature on measurements of extensional viscosity with the opposed-nozzle device. The effect of liquid inertia is addressed with experiments on Newtonian liquids and by solving the Navier-Stokes equations. The effect of the ratio of nozzle separation to nozzle diameter on measured apparent extensional viscosity is investigated with experiments on three Newtonian liquids of different viscosities. A simple analysis of the effect of nozzle separation on the total strain is presented and the limitations of the assumption of extensional flow kinematics are examined. Lastly, use of the opposed-nozzle device as an extensional indexer is examined using a series of polymer solutions.

Experimental

Pure glycerin, from Milsolv Co., and several glycerin-water mixtures, denoted as liquids A–E, were used as test Newtonian liquids (see Table 2). Aqueous poly(ethylene oxide) (PEO) solutions were used as model semi-dilute solutions of flexible coils in a good solvent. PEO was obtained from Polysciences Inc. and its molecular weight was reported by the manufacturer to be 5 Mg/mol. A stock solution containing 1.89% by weight PEO in distilled water was prepared by slowly adding the polymer to a stirrer-induced vortex in water in a continuously stirred tank. A flat blade stirrer rotating at about 1000 rpm was chosen to reduce chain scission. The solution was stirred for 24 h and allowed to stand for a few days to homogenize completely. Portions of the stock solution were then diluted with distilled water to prepare 250 ml solutions with 0.05%, 0.13%, 0.38%, 0.63%, 0.95%, 1.26%, and 1.89% PEO concentration by weight.

Table 1 Measurements reported in literature on extensional viscosity of Newtonian liquids in opposed-nozzle devices

Author	$\frac{h}{R}=1$	R (mm)	η_S (Pa s)	$\dot{\varepsilon}$ (s^{-1})	η_E (Pa s)	T_A	Notes
Fuller et al. (1987)	✓	0.5	0.248	400–2800	0.56–0.9	2.25–3.6	$0.25 \leq \frac{h}{R} \leq 1.4$; lower η_E at larger $\frac{h}{R}$
		0.5	0.12	1200–4200	0.35–0.42	2.9–3.5	
Mikkelsen et al. (1988)	✓	0.25	0.012	1000–20000	0.055–0.103	4.6–8.6	$0.5 \leq \frac{h}{R} \leq 2$; lower η_E at larger $\frac{h}{R}$
Schunk et al. (1990)	✓	0.5	0.17	80–2500	0.51–0.62	3–3.65	Data from Mikkelsen (1989), private communication
Laun and Hingmann (1990)	✓	0.5	1.2	50–500	3.6–4.7	3–3.9	η_S estimated, pure glycerin, 23 °C
		0.5	0.45	300–1500	1.35–1.6	3–3.6	η_S estimated, 95% glycerin-water, 23 °C
		0.5	0.19	250–3000	0.51–0.74	2.7–3.9	η_S estimated, 90% glycerin-water, 23 °C
Cai et al. (1992)	✓	0.25–2.5	0.027	1–30000	0.08–0.3	3–11	
Anklam et al. (1994)	✓	0.5–1	1	50–800	3.1–3.5	3.1–3.5	
Hu et al. (1994)	✓	0.5–2.5	0.081	5–1000	0.22–0.29	2.7–3.6	
		0.5–2.5	0.038	5–1000	0.11–0.17	2.9–4.5	
Hermansky and Boger (1995)	✓	0.25	0.156	500–8000	0.42–0.56	2.7–3.6	η_E approximately insensitive to $\frac{h}{R}$ in $0.7 \leq \frac{h}{R} \leq 2$ then decreases at larger ratios
		0.25	0.110	500–8000	0.25–0.35	2.25–3.15	
		0.25	0.077	1000–17000	~0.23	~3	
		0.25	0.030	1000–20000	~0.09–0.24	~3–8	
		0.25	0.0105	1000–20000	~0.032–0.18	~3–17	
		0.25	0.0055	1000–20000	~0.017–0.17	~3–30	
		0.25	0.0036	5000–20000	0.054–0.22	15–60	
		0.25	0.0010	5000–20000	0.035–0.15	35–150	
		0.5	0.0010	2200–10000	0.047–0.29	47–290	
		1	0.0010	600–1400	0.055–0.42	55–420	

Shear viscosities of all liquids were measured with a Rheometrics RFS-II controlled strain rheometer equipped with a transducer capable of measuring torques greater than 0.002 g cm (0.196 μN m). Glycerin is hygroscopic, and its viscosity varies strongly with temperature and water content (Newman 1968). Hence, a flooded Couette geometry with cup diameter 34 mm, bob diameter 32 mm and bob length 33 mm was used for the Newtonian liquids. Shear viscosities of PEO solutions were measured with a cone and plate fixture with a small-angle cone of 0.021 rad and diameter 50 mm, and a gap of 48 μm between the cone and plate. These fixtures were covered with water-soaked foam-lined covers to avoid evaporation of water from the solutions.

Table 2 Properties of glycerin-water mixtures used as Newtonian liquids in this study

Liquid	Approximate vol. fraction glycerin[b]	Density[a] [kg/m^3]	Shear viscosity [mPa s]	Temperature [°C]
A	1	1260	770	24±0.5
B	0.92	1240	345	24±0.5
C	0.79	1204	56	21±0.5
D	0.57	1148	11	21±0.5
E	0	1000	1.1	21±0.5

[a] Measured with calibrated hydrometers.
[b] Glycerin samples were exposed to atmosphere before tests. Water content may be higher than reported

Extensional viscosity measurements were made with a Rheometrics RFX indexer using the opposed-nozzle configuration with six pairs of nozzles of 5, 4, 3, 2, 1 and 0.5 mm in diameter. Smaller nozzles were used to generate higher apparent extension rates at a same given liquid flow rate. The smallest nozzles, 0.5 mm in diameter, were used only with low viscosity liquids in order to verify Hermansky and Boger's (1995) observations at high strain rates. These measurements were found to be very sensitive to alignment of the nozzles, and hence this nozzle size was not used in later measurements. The temperature was maintained constant in the opposed-nozzle device with a temperature-controlled bath connected to a jacketed glass beaker containing the test liquid. Measurements were made at 21±0.5 °C except where noted.

Apparent extensional viscosity measurements were made when the torque signal, indicated by a chart recorder, reached steady state. An example of the chart recorder trace for liquid A is shown in Fig. 3. The torque initially grows with time and may show an overshoot (with elastic solutions) before reaching a nearly constant value. The time during which the torque approaches its steady value varies with nozzle diameter, apparent extension rate, and liquid being tested. Elastic PEO solutions showed longer transients than Newtonian liquids at the same apparent extension rate. These ranged from 120 s

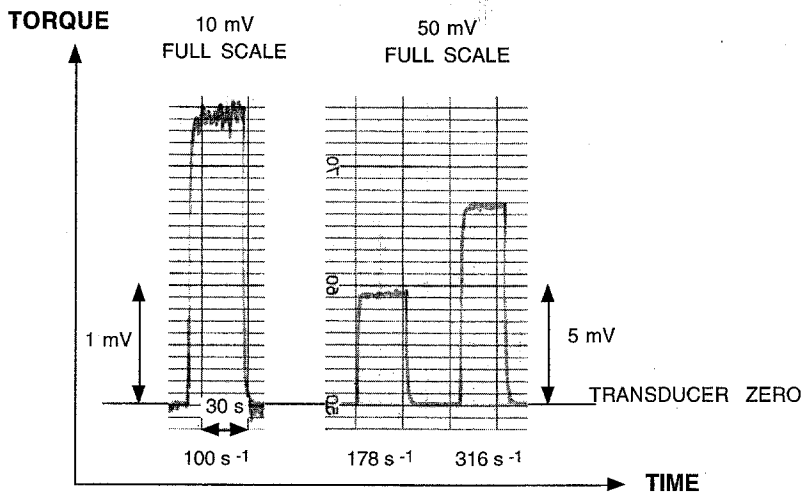

Fig. 3 Chart recorder trace showing the variation of torque as a function of time with glycerin for three successive apparent extension rates of 100, 177.8 and 316.2 s^{-1}. The abscissa scale is 2 cm *chart travel*/min. A finite rise time during which the torque approaches a steady value can be seen even for Newtonian liquids. This rise time comprises the "delay time" of the instrument

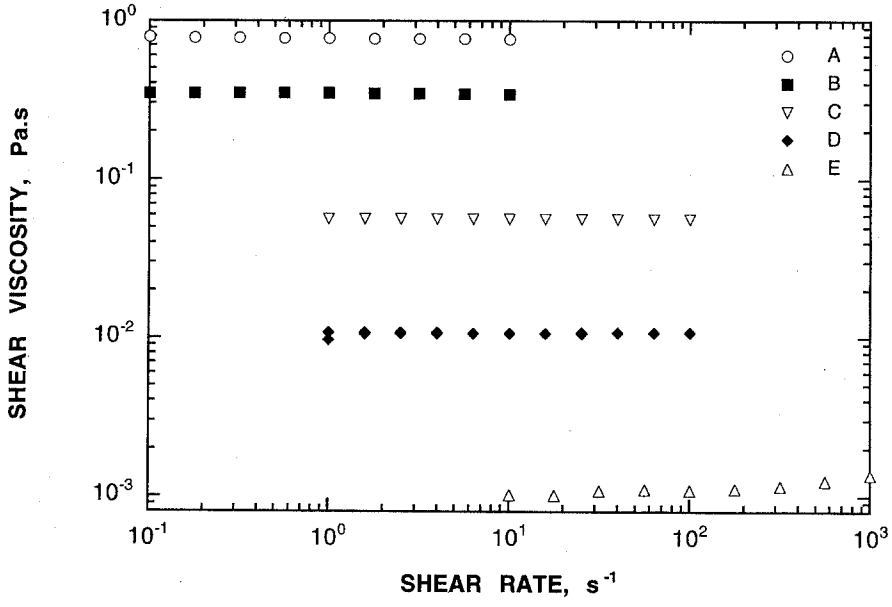

Fig. 4 Shear viscosity of Newtonian test liquids A–E (Table 2). All measurements were made with a flooded Couette geometry using a Rheometrics RFS-II rheometer

at lower rates with each nozzle to about 10 s at higher rates. Test times, during which the torque was measured, varied between 5 and 10 s. Delay times used with elastic PEO solutions were longer than those of the Newtonian liquids at the same apparent extension rate. All measurements were made with a nozzle diameter-to-separation distance ratio of unity (Schunk et al., 1990), except when the effect of nozzle separation in Newtonian liquids was tested. Approximately three decades in apparent extension rate could be tested with each nozzle pair. However, Mikkelsen et al. (1988) and Schunk et al. (1990) report data which deviate with increasing Reynolds number (approximately greater than 2). Hence measurements were made at Reynolds numbers less than about unity except with the low viscosity liquids C, D and E. This constraint, coupled with the smallest measurable torque limit, permitted only slightly more than a decade in apparent extension rate to be tested with each nozzle size. Ranges covered by successive nozzle sizes overlap, and the difference in viscosity measured with two nozzle sizes is used to identify artifacts related to the instrument or to the measurement technique. Viscosities of both Newtonian liquids and PEO solutions measured at the same rate with different nozzle sizes were found to agree to within 10%.

Newtonian liquids – general trends

Figures 4 and 5 show the shear and apparent extensional viscosity of the Newtonian liquids used in the study. Shear viscosities ranged from 1 to 776 mPa s.

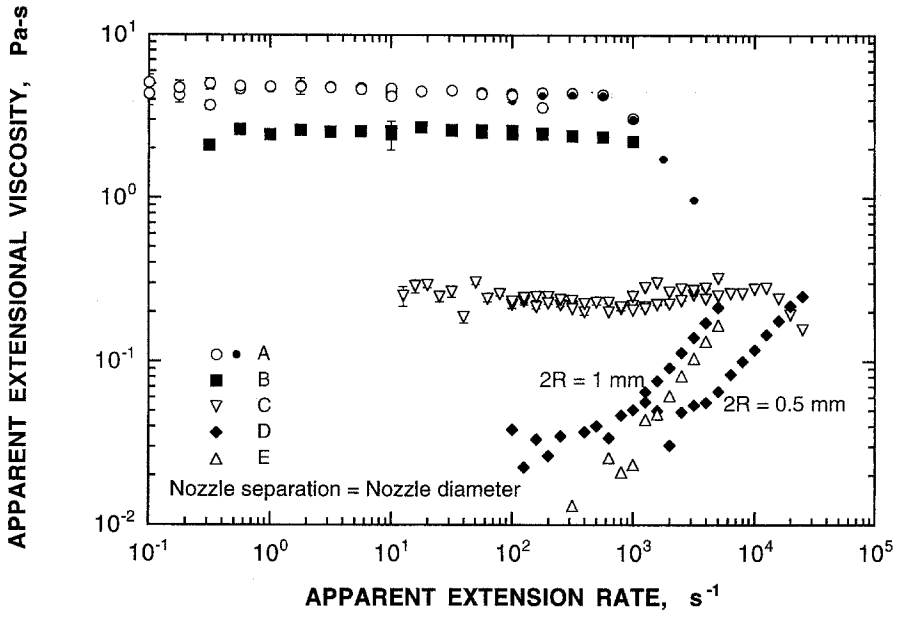

Fig. 5 Apparent extensional viscosities of liquids A–E. Filled symbols in case of liquid A denote repeated measurements. Liquids A, B, and C show a fairly constant extensional viscosity over a wide range of apparent extension rates. The lower viscosity liquids D and E show a sharp rise in measured viscosity with extension rate. Measurements on liquid D show a strong dependence on nozzle diameter

Reproducibility of the apparent extensional viscosity measurements is indicated by the repeated runs with the 1 mm diameter nozzles on liquid A. Successive measurements on liquid A at the same apparent extension rate with different nozzles, e.g. in Fig. 5 at 10 s^{-1} with 2, 3 and 4 mm diameter nozzles, also agree to within less than 10%. The apparent extensional viscosity of liquid A is about 5.5 times its shear viscosity; that of liquid B is about 7 times it shear viscosity. With these two liquids the highest Reynolds number ($\mathrm{Re} \equiv \frac{\rho Q h}{\eta_S \pi R^2}$) achieved was around unity at all nozzle diameters used. The apparent extensional viscosity of liquid C is also approximately constant, and about 4.5 times its shear viscosity. The data from different nozzles show first a slight downturn and then upturns at high rate ($\mathrm{Re} \approx 10$). This upturn is discussed below in conjunction with the apparent extensional viscosities of liquids D and E.

Apparent extensional viscosities of lower viscosity liquids, i.e. liquids D and E, were measured at higher Reynolds numbers with 1 and 0.5 mm nozzles. The lower limits of extension rate tested with these low viscosity liquids were set by the sensitivity of the torque transducer. Whereas the apparent extensional viscosity of liquid C is approximately constant, like that of liquids A and B, that of liquids D and E rises sharply with apparent extension rate. This rise was also reported by Hermansky and Boger (1995). These measurements are also sensitive to nozzle diameter as shown by the data on liquid D with the 1 and 0.5 mm diameter nozzles; this sensitivity of very low viscosity liquids was also reported by Hermansky and Boger (Fig. 6 of their paper). Measurements with water (liquid E) with 0.5 mm nozzle showed significant scatter because of low torques and could not be reproducibly measured. Figure 6 shows the same data plotted against Reynolds number ($\mathrm{Re} = \frac{\rho \dot{\varepsilon} h^2}{\eta_S}$). Apparent extensional viscosity of liquid D was roughly constant at low rates with the 1 mm nozzles, and then sharply rose at $\mathrm{Re} \approx 10$ and higher. Data from both 1 mm and 0.5 mm nozzles are nearly similar at these higher Reynolds numbers. Only the sharp rise was observed with water (liquid E) at the Reynolds numbers tested.

These observations suggest that opposed-nozzle devices can measure the extensional behavior of liquids at Reynolds numbers less than unity. At higher Reynolds numbers, viscous dissipation in the entire flowing liquid and other effects could become important and may cause the apparent viscosity to rise (see next section). Also, the apparent extensional viscosity of Newtonian liquids whose shear viscosities are less than about 50 mPa s cannot be reliably measured with the RFX due to combination of transducer sensitivity and high Reynolds number effects.

Effect of high flow rates

Experimental

The apparent extensional viscosity of liquid A in Fig. 5 falls sharply at strain rates higher than 560 s^{-1}. Frequent limitations of the opposed nozzles device with high viscosity liquids are that the liquid may cavitate under the low pressure in the syringes during the experiment, or that air may leak into the syringes if they are not well-sealed at the joints. In either case, the measured force re-

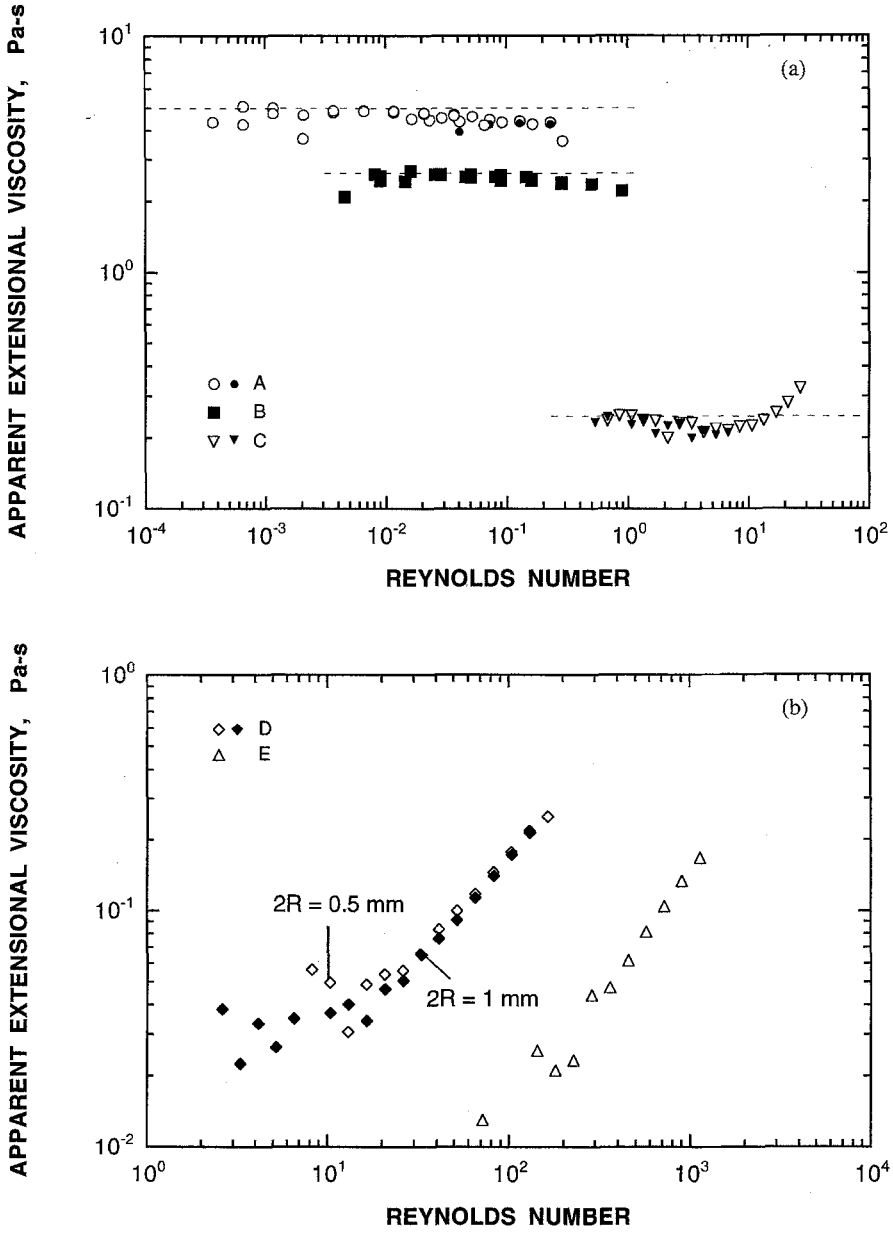

Fig. 6 Apparent extensional viscosities of (a) liquids A–C, and (b) liquids D and E versus Reynolds number ($\frac{\rho \dot{\varepsilon} h^2}{\eta_s}$). Filled symbols in case of liquids A and C denote repeated measurements. Viscosities of liquids A and B are fairly constant. Data on liquid C taken with 1 mm diameter nozzles only is plotted for clarity. Viscosity of liquids D and E increase with Reynolds number. Viscosity of liquid D does not depend on nozzle radius when plotted against Reynolds number, unlike when plotted against extension rate in Fig. 5

mains approximately constant, and the apparent extensional viscosity falls with a slope of –1 with apparent extension rate on a log-log plot. This can be seen in the data from liquid A at apparent extension rates greater than 10^3 s^{-1} (Fig. 5). Cavitation can be delayed by degassing the liquids (Willenbacher and Hingmann, 1994); air leaks can be delayed by greasing the syringes and joints.

A slight downward trend in measured viscosity of solution A is seen between 560 and 1000 s^{-1}, just before air leaks into the syringes, and also appears in the measurements on liquid B with the 1 mm nozzle at apparent extension rate of about 300 s^{-1} ($Re \approx 0.2$ in Fig. 6a). At least two factors may concur to lower the extensional viscosity measurements. When liquid is sucked, axial viscous stresses pull the nozzles together, whereas convective flux of momentum (inertia) and shear forces on nozzle walls push them apart (see following section). At higher extension rates and consequently higher flow rates, the influence of momentum flux is greater. Also, vortices in the surrounding liquid may become more intense, causing higher shear forces on the nozzle walls. A similar incipient trend in the data on liquid A is evident at apparent extension rates of about 100 s^{-1} with the 2 mm nozzles (Fig. 5).

Apparent extensional viscosities of the lowest viscosity liquids D and E, with shear viscosities 11 and

1 mPa s, increase strongly with strain rate. The measured apparent extensional viscosities exceed up to 100 times the shear viscosities, in agreement with the observations of Hermansky and Boger (1995), but this phenomenon *cannot be attributed to liquid inertia.*

Analysis

Hermansky and Boger (1995) propose an empirical correction to correct for liquid inertia. However, the effect they corrected for is not due to liquid inertia, and may be a consequence of the accompanying flow in the test liquid outside the extensional flow volume. Moreover, their evaluation of the empirical constant introduced in their analysis is flawed, as explained in the Appendix.

Pasquali and Scriven (1996) reported the following contributions to the measured torque in the opposed-nozzle device:

$$\eta_E\dot{\varepsilon} \equiv \underbrace{\frac{f_R}{\pi R^2}}_{\substack{\text{measured}\\ \text{force/area}}} = \underbrace{\eta_U\dot{\varepsilon}(1+2\ln b)}_{\substack{\text{losses in the}\\ \text{extensional flow}\\ \text{per unit flow rate}}} - \underbrace{\frac{2L}{R}\bar{\tau}_{rz}}_{\substack{\text{mean shear stresses}\\ \text{on nozzle surface}}} - \underbrace{\frac{7}{16}\rho\dot{\varepsilon}^2h^2}_{\text{inertia}} + \underbrace{\frac{\dot{C}_{m,NE}}{2Q}}_{\substack{\text{losses in the rest}\\ \text{of the device}\\ \text{per unit flow rate}}} . \tag{7}$$

Here η_U is the liquid's *true* extensional viscosity (Eq. (4)), f_R is the measured force, R is the nozzle radius, $b \equiv R_0/R$ is the ratio between the unknown radial location R_0 of the inflow surface and the nozzle radius, L is the length of the nozzle, $\bar{\tau}_{rz}$ are average shear stresses on the nozzle lateral surface, h is half the nozzle separation, Q is the flow rate into each nozzle and $\dot{C}_{m,NE}$ are losses of mechanical energy due to viscous dissipation *outside* the extensional flow volume V_E (see Figs. 1 and 2). Equation (7) was derived from a balance of linear momentum on a control surface $S_L + S_N$ around the nozzle *up to the nozzle face*, as depicted in Fig. 2. Equation (7) shows that inertia is not the only extraneous contribution to the torque measurement. The analysis of Pasquali and Scriven also shows that the effect of inertia is tightly connected to that of the dynamic pressure at the nozzle face.

The inertial term is

$$\mathcal{I} \equiv \frac{1}{\dot{\varepsilon}\pi R^2}\boldsymbol{e}_z \cdot \int_S \boldsymbol{n}\cdot\boldsymbol{v}\rho\boldsymbol{v}dS \tag{8}$$

where $\boldsymbol{n}$ is the normal to surface S and $\boldsymbol{e}_z$ is the axial unit normal. $\mathcal{I}$ can be evaluated either at the nozzle face S_N (Eq. (7)) or on the cylindrical surface S_c between the nozzles (Fig. 2, also Schunk et al., Fig. 2). Schunk et al. (1990) showed that the choice of the latter surface is optimal in the sense of maximizing the contribution of the extensional stresses on the total measured torque. Therefore any *quantitative* inertia correction should be evaluated on control surface S_c. Anklam et al. (1994, p. 809) proposed to use simple extensional flow kinematics (Eq. (3)) to evaluate the effect of inertia on surface S_c. Doing so leads to

$$\eta_{\text{inertia}} \equiv \frac{1}{\dot{\varepsilon}\pi R^2}\int_{S_c}\rho v_r v_z dS = \frac{1}{\dot{\varepsilon}\pi R^2}\int_0^{2\pi}d\theta\int_0^h\left(-\dot{\varepsilon}\frac{R}{2}\right)\rho(\dot{\varepsilon}z)dz = -\frac{\rho h^2\dot{\varepsilon}}{2} . \tag{9}$$

Anklam et al. (p. 809) correctly pointed out that "inertia *opposes* the force due to the fluid extension"; therefore the magnitude of the inertia contribution should be *added* to the measured extensional viscosity, not subtracted as in Eq. (5).

In order to assess the validity of Eq. (9), the flow of a Newtonian liquid around a nozzle was found by solving the Navier-Stokes equation system with Galerkin's method of weighted residuals and finite elements basis functions. The solution method, boundary conditions and geometry were those used by Schunk et al. (1990). The calculations were made with the commercial software Nekton Version 3.0 from Fluent Inc. (1995).

Figure 7 shows that the assumption of extensional flow kinematics on surface S_c does not provide a reasonable approximation to the velocity computed by solving the Navier-Stokes equations. The Reynolds number is defined as

$$\text{Re} \equiv \frac{\rho Qh}{\eta_S\pi R^2} = \frac{\rho\dot{\varepsilon}h^2}{\eta_S} . \tag{10}$$

Figure 8 compares the values of the flux of z-momentum, $\rho v_z v_r$ (normalized by $\rho\dot{\varepsilon}^2 h\frac{R}{2}$) through surface S_c as functions of axial position calculated by Navier-Stokes analysis and by assuming extensional flow kinematics. Simple extensional flow (Eq. (3)) leads to a large overprediction of the momentum flux into the control volume, and that in turn overestimates the inertia correction. Table 3 compares the inertia correction $\mathcal{I}_{NS}$ calculated by the Galerkin-Finite Element solution of the Navier-Stokes equations with that obtained by assuming simple extensional flow in the control volume, $\mathcal{I}_{Ext}$. The former is

$$\mathcal{I}_{NS} \equiv \frac{1}{\dot{\varepsilon}\pi R^2}\int_{S_c}\rho v_r v_z dS \tag{11}$$

where v_r and v_z are respectively the calculated radial and axial velocity components on the surface S_c. The latter is Eq. (9). The inertia correction calculated by Navier-Stokes analysis is about 30% of that given by

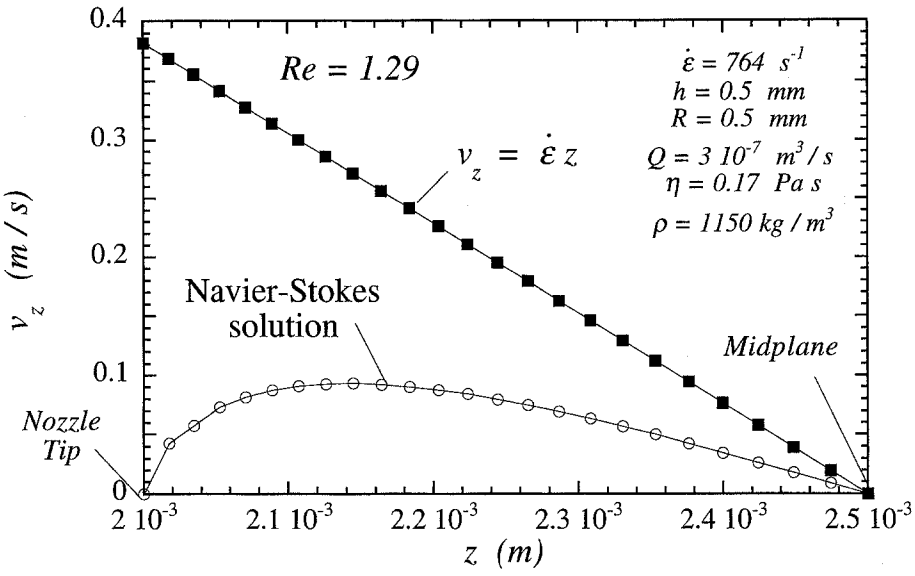

Fig. 7 Calculated axial velocity v_z on control surface S_c at Reynolds number Re=1.29. Open symbols are solutions of Navier-Stokes equations. Filled symbols are obtained by assuming simple extensional flow, i.e. $\boldsymbol{v} = \dot{\varepsilon} z \boldsymbol{e}_z - \dot{\varepsilon}\frac{r}{2}\boldsymbol{e}_r$. The velocities predicted with this assumption are much higher than those calculated by Navier-Stokes analysis. This is due to the no-slip condition enforced at the nozzle tip ($z=2{\cdot}10^{-3}$ m). Virtually identical results are obtained at Re=0.129 and Re=12.9. (The sign of all velocities has been reversed for convenience)

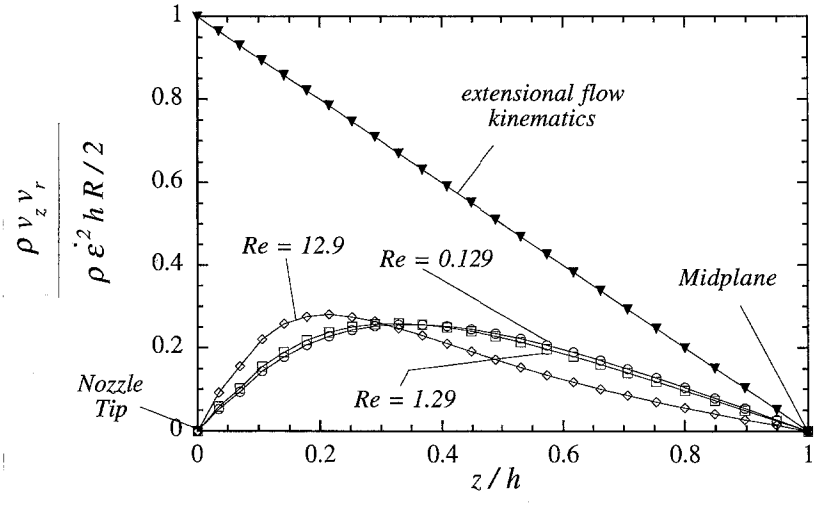

Fig. 8 Calculated normalized momentum flux $\frac{\rho v_z v_r}{\rho \dot{\varepsilon}^2 h R/2}$ on control surface S_c at different values of Reynolds number. Open symbols are solutions of Navier-Stokes equations. Filled symbols are obtained from extensional flow kinematics. The fluxes predicted by assuming simple extensional flow are much higher than those calculated by Navier-Stokes analysis. The normalized profiles show little difference at low and moderate Reynolds numbers. The area under the curves is the total contribution of inertia to the measured torque and is roughly independent of Reynolds number

Eq. (9), and the ratio $\mathcal{I}_{NS}/\mathcal{I}_{Ext}$ is fairly insensitive to Reynolds number. Therefore the following inertia correction arises in the range of Reynolds number investigated here at $h/R=1$:

$$\eta_E = \eta_{\text{measured}} + 0.3\,\frac{\rho h^2 \dot{\varepsilon}}{2}\,, \quad \text{or} \tag{12}$$

$$T_A = T_{\text{measured}} + 0.15\,\text{Re} \quad \text{for } 0.1 \le \text{Re} \le 10\,, \quad \frac{h}{R} = 1\,. \tag{13}$$

Finally, Eq. (7) of this paper and Fig. 8 of Schunk et al. (1990) show that a correction based on the inertia of the liquid alone is not appropriate because other terms of comparable magnitude contribute to the total force measured, too. There appears to be no theoretical way, other than solving the Navier-Stokes system, to account for the effect of shear stresses and losses outside the extensional control volume.

Table 3 Comparison between inertia contribution by solving the Navier-Stokes equations and by assuming extensional flow kinematics

Reynolds number Re	Inertia[a] (Navier-Stokes) $\mathcal{I}_{NS}$ Eq. (11)	Inertia[a] (extensional flow) $\mathcal{I}_{Ext}$ Eq. (9)	$\frac{\mathcal{I}_{NS}}{\mathcal{I}_{Ext}}$
0.129	0.1619	0.5	0.3238
1.29	0.1604	0.5	0.3209
12.9	0.1449	0.5	0.2899

[a] $\mathcal{I}$ made dimensionless by $\rho h^2 \dot{\varepsilon}$

Equation (12) predicts that the effects of inertia should be observed at lower apparent extension rates with lower viscosity liquids. This agrees with the experiments on liquids A and B shown in Fig. 5. The inertia contribution calculated with Eq. (12) is always less than 1% of the measured apparent extensional viscosity of pure glycerin, and less than 10% of the measured apparent extensional viscosity of the glycerin-water solution.

Even though Eq. (12) has been derived under clear hypotheses, using it to correct measurements of extensional viscosity quantitatively *is not recommended* because the correction accounts only for one of several extraneous contributions to the apparent viscosity measurements. Moreover, Eq. (12) predicts that the measured apparent extensional viscosity of a Newtonian liquid should fall with rising extension rate. This effect is small and usually seen only over a narrow range of extension rates, whereas the measured apparent extensional viscosity usually rises with extension rate at high rates (Figs. 5 and 6). No quantitative conclusions can be drawn from Eq. (7) because shear stresses on the nozzle walls and viscous dissipation in the entire volume of flowing liquid can not be quantified under the simplifying assumptions of extensional flow kinematics.

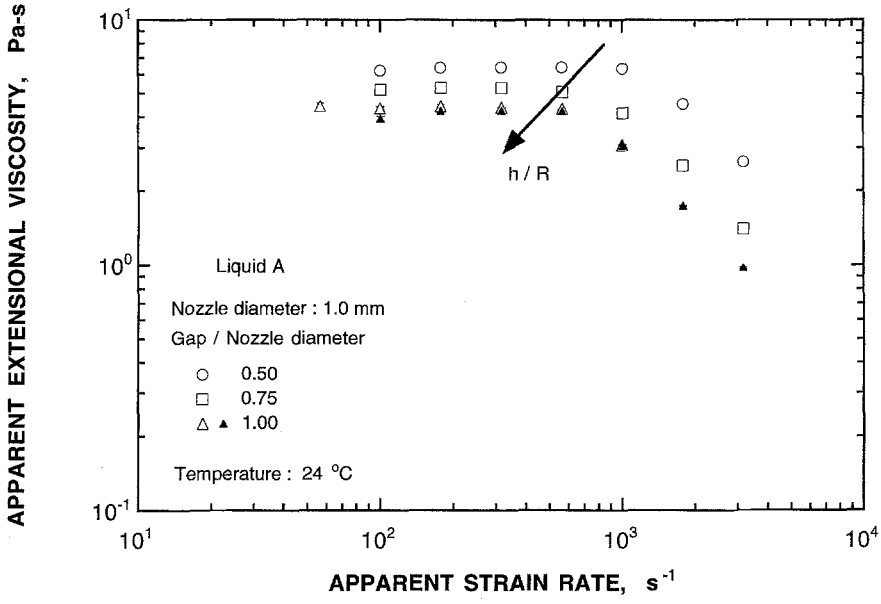

Fig. 9 Effect of nozzle separation on the apparent extensional viscosity of liquid A measured with 1 mm diameter nozzles. The measured viscosity falls as the nozzles are separated

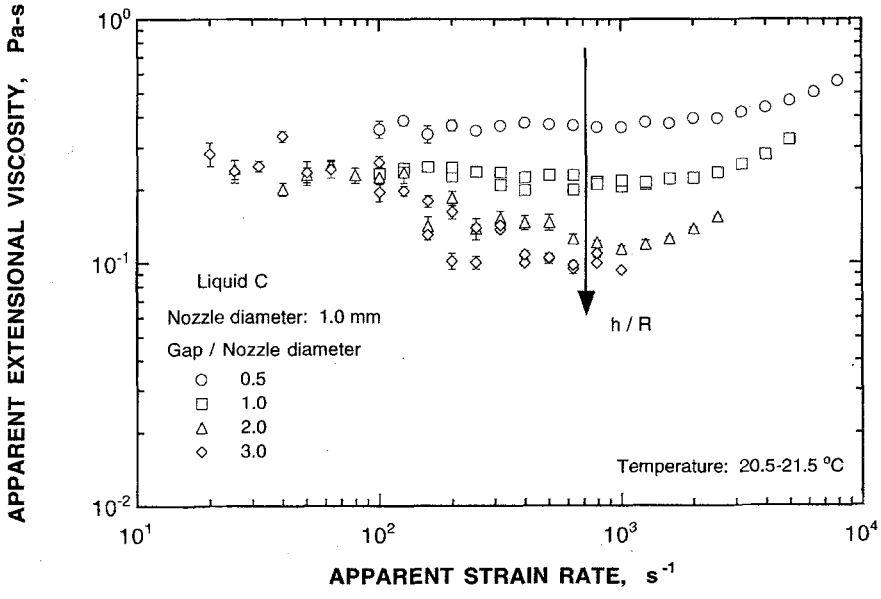

Fig. 10 Effect of nozzle separation on the apparent extensional viscosity of liquid C measured with 1 mm diameter nozzles. The measured viscosity falls as the nozzles are separated

Effect of separation between nozzles

Experimental

Figures 9–11 demonstrate the effect of varying nozzle separation on measured apparent extensional viscosity of the Newtonian liquids A, B, C. The apparent viscosity of liquid A *falls* if the nozzle separation is *increased* at constant nozzle diameter $2R=1$ mm (Fig. 9). Similar behavior is displayed by liquid C (Fig. 10).

The measured apparent extensional viscosity of liquid B is fairly insensitive to nozzle separation at nozzle diameter $2R=1$ mm (Fig. 11 a). It *rises* slightly with *increasing* gap at nozzle diameter $2R=4$ mm (Fig. 11 b).

These limited tests show that changing the nozzle separation can either raise or lower the measured extensional viscosity of Newtonian liquids, depending on both liquid viscosity and nozzle diameter. Once more this reflects the presence of extraneous contributions to the force measurement. The relative importance of these contributions need not be constant if the ratio of gap to diameter is varied (Schunk et al., 1990, Figs. 8 and 9).

Schweizer et al. (1990) reported that the effective extensional viscosity of M1 increased with nozzle separa-

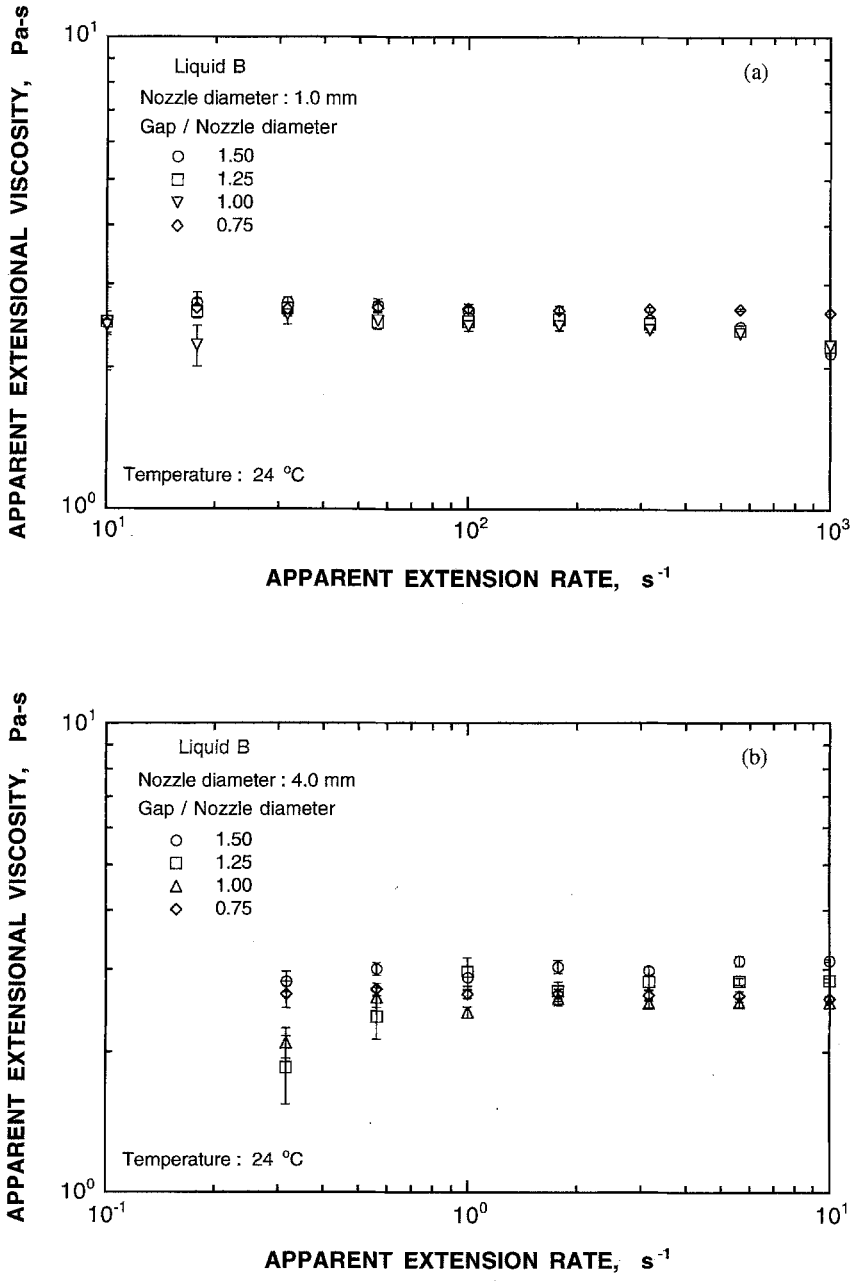

Fig. 11 Effect of nozzle separation on the apparent extensional viscosity of liquid B measured with (a) 1 mm diameter nozzles, and (b) 4 mm nozzles. The measured viscosity is fairly insensitive to nozzle separation in (a) but rises as nozzles are separated in (b)

tion and attributed this phenomenon to longer average residence times in the flow and therefore to the higher total strains. Willenbacher and Hingmann (1994) observed similar behavior with S1. As discussed next, the dependence of average residence time of the liquid in the flow on gap cannot be predicted by assuming simple extensional flow kinematics. The extent of liquid involved in the extensional flow should be visually determined to check whether the residence time is really influenced by nozzle separation (see Eq. (19) in the following section).

Analysis

One of the uncertainties in the analysis of RFX data is the residence time of the liquid elements in the extensional flow field. Cathey and Fuller (1990, p. 81) stated that the average residence time $\bar{t}_R$ of an element, calculated under the assumption of simple extensional flow kinematics (Eq. (3)), is $\bar{t}_R = \frac{1}{\dot{\varepsilon}}$, and that the average strain imposed on the material is then $\bar{\varepsilon} \equiv \dot{\varepsilon}\bar{t}_R = 1$. Willenbacher and Hingmann (1994, p. 172) argued in a subsequent article that the average strain is a rising function of the ratio of nozzle separation to diameter $2h/2R$, but they did not report a derivation or a formula for the average strain. The Rheometrics RFX owner's manual (1991) records the following relationship:

$$\bar{t}_R = \frac{1}{\dot{\varepsilon}}\left(1 + \ln\frac{h}{R}\right). \tag{14}$$

This supports the claims that the average residence time can be lengthened by raising the ratio of nozzle gap to diameter.

The residence time t_R of a fluid particle in a flow field is given by

$$t_R \equiv \int_{y_0}^{y} \frac{1}{v} ds \tag{15}$$

where $\boldsymbol{y}_0$ and $\boldsymbol{y}$ are the position vectors of the fluid particle at the inflow and outflow surfaces, v is the magnitude of the velocity vector, s is the arclength along the streamline and the integral is calculated along the streamline. The velocity in uniaxial extension is given by Eq. (3) and the streamlines are described by $zr^2 = k$. A fluid particle occupying the position $\boldsymbol{y}_0 \equiv z_0\boldsymbol{e}_z + r_0\boldsymbol{e}_r$ at time t_0 occupies the position $\boldsymbol{y}(t)$ at time t:

$$\boldsymbol{y}(t) \equiv z(t)\boldsymbol{e}_z + r(t)\boldsymbol{e}_r = z_0 e^{\dot{\varepsilon}(t-t_0)}\boldsymbol{e}_z + r_0 e^{\frac{-\dot{\varepsilon}(t-t_0)}{2}}\boldsymbol{e}_r . \tag{16}$$

Conversely, a material element moves from $\boldsymbol{y}_0$ to $\boldsymbol{y}$ in a time

$$t_R(r) = \frac{1}{\dot{\varepsilon}}\ln\frac{z}{z_0} = -\frac{2}{\dot{\varepsilon}}\ln\frac{r}{r_0} \tag{17}$$

The average residence time $\bar{t}_R$ of the liquid in the extensional flow field between opposed nozzles is defined as

$$\bar{t}_R \equiv \frac{1}{S}\int_{S_N} t_R(S)dS \tag{18}$$

where $S \equiv \pi R^2$ is the area of the nozzle face S_N (Fig. 1), and R is the nozzle's radius. Equations (17) and (18) give

$$\begin{aligned}\bar{t}_R &= \frac{1}{\pi R^2}\int_0^{2\pi} d\theta \int_0^R t_R(r) r dr = \frac{2}{R^2}\int_0^R -\frac{2}{\dot{\varepsilon}}\ln\frac{r}{R_0} r dr \\ &= -\frac{4R_0^2}{\dot{\varepsilon}R^2}\int_0^{R/R_0} \xi \ln\xi d\xi = \frac{1}{\dot{\varepsilon}}\left(1 + 2\ln\frac{R_0}{R}\right) \\ &= \frac{V_E}{2Q} .\end{aligned} \tag{19}$$

Equation (19) shows that the average residence time, and therefore the average strain $\bar{\varepsilon} \equiv \dot{\varepsilon}\bar{t}_R$, depends on the location R_0 of the inflow surface (see Fig. 2) of the extensional control volume V_E, that is, on the size of the extensional control volume. This location cannot be evaluated from the hypothesis of simple extensional flow. The value of $\bar{t}_R$ cannot be extrapolated by assuming "infinitely far" inflow because the average residence time becomes infinite if $R_0 \to \infty$. The formula reported in the RFX owner's manual (Eq. (14)) is not valid unless $R_0 \approx \sqrt{hR}$; if the rule of thumb $h = R$ is used, then this implies that liquid enters the extensional flow at a radial coordinate R_0 comparable with the nozzle radius R. The claims of Schweizer et al. (1990) and Willenbacher and Hingmann (1994) that the gap-to-diameter ratio affects the average residence time of the liquid elements cannot be explained by assuming simple extensional flow; nonetheless their assertion may be correct.

The size of the extensional flow volume must be estimated by flow visualization or by solution of the full set of partial differential equations governing the flow. The latter approach requires appropriate boundary conditions and constitutive equations, which are not readily available for most non-Newtonian liquids. As a final remark, the ratio $b \equiv R_0/R$, that is the magnitude of the extensional flow volume, affects the apparent viscosity measurement too (Eq. (7)), regardless of the kind of liquid investigated (elastic or not). To the authors' knowledge, no systematic experimental or theoretical study has been conducted on the relationship between R_0 and h, that is between the volume of liquid in the extensional flow and the nozzle separation.

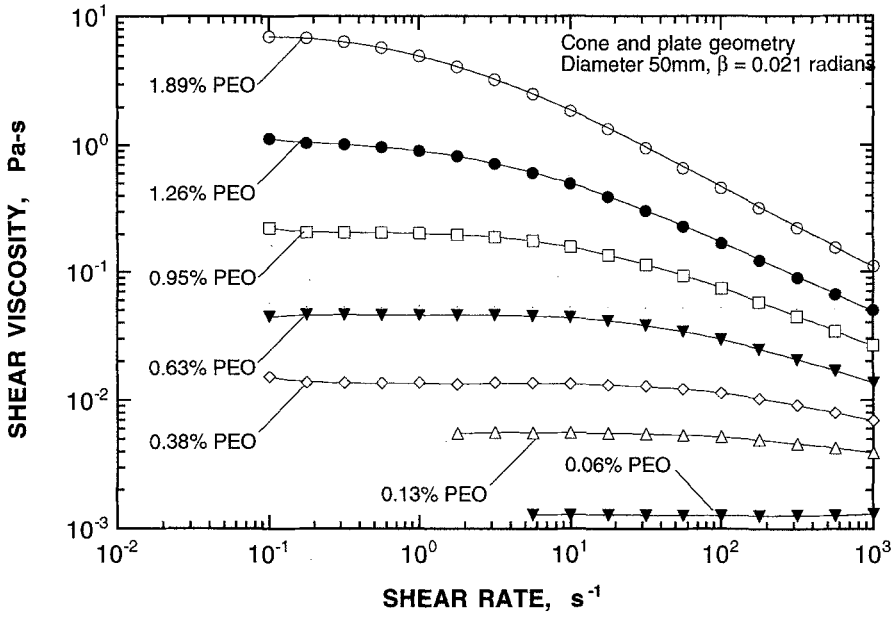

Fig. 12 Steady shear viscosities of poly(ethylene oxide) solutions in water at various concentrations (M_w=5 Mg/mol) measured with a cone-and-plate fixture in a Rheometrics RFS-II rheometer

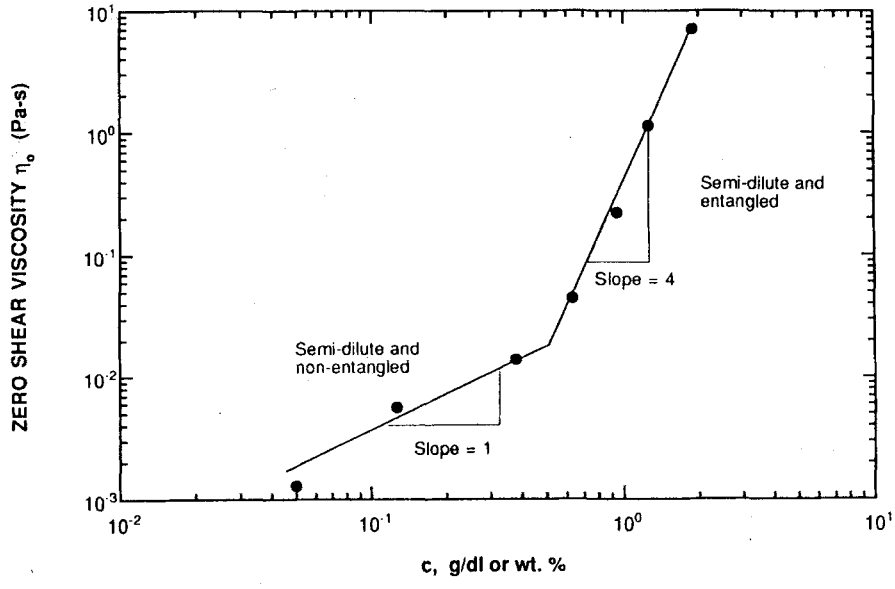

Fig. 13 Variation in zero-shear viscosity, η_0, with concentration for the polymer solutions shown in Fig. 12. The asymptotic behavior $\eta_0 \sim c$ at lower concentrations indicates absence of entanglements. The asymptotic behavior $\eta_0 \sim c^4$ shows the effects of entanglements at higher concentration

Polymer solutions

Shear viscosities

The steady shear viscosities of solutions of 0.06%, 0.13%, 0.38%, 0.63%, 0.95%, 1.26% and 1.89% by weight PEO in water are shown in Fig. 12. The viscosity rises and the shear-thinning behavior intensifies with polymer concentration. Figure 13 shows the zero-shear viscosity of the same solutions as a function of polymer concentration. The zero-shear viscosity first grows linearly with concentration at low concentrations and then with the fourth power at high concentrations. Solutions up to about c=0.5% are not entangled, while those above are entangled. This concentration can not be precisely defined because the PEO sample was polydisperse, and degraded in the intense shear field while the solution was being mixed.

Extensional viscosities

Figure 14 compares the apparent extensional viscosity of five solutions ranging in concentration from 0.38% to 1.89% PEO. Whereas the shear viscosity drops with rising shear rate, the apparent extensional viscosity

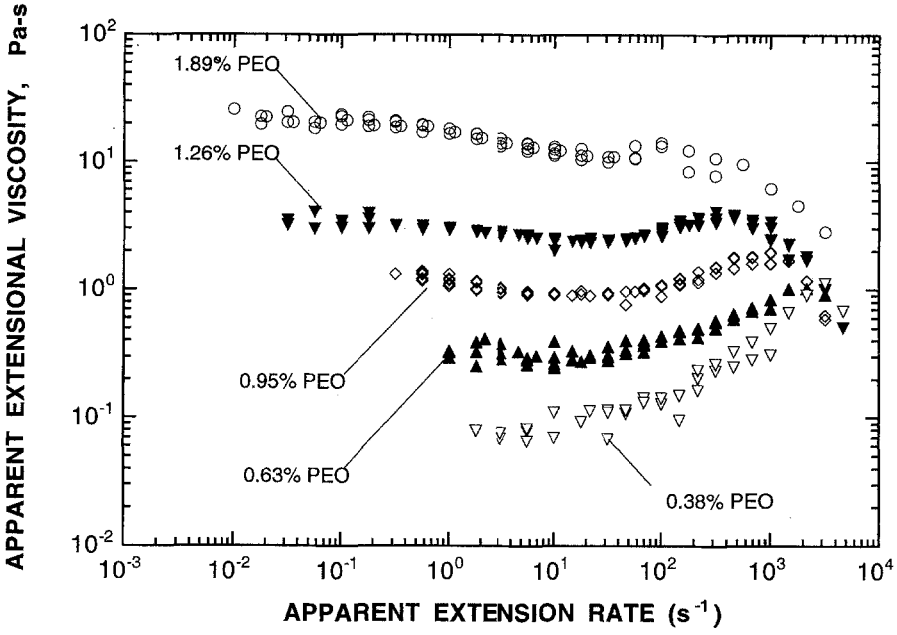

Fig. 14 Apparent extensional viscosities of the poly(ethylene oxide) solution in water shown in Fig. 12, ranging from 0.38 to 1.89wt%. Torque levels of the remaining solutions at lower concentration were below transducer specifications

drops slightly initially and then climbs with apparent extension rate. The onset of extension-thickening behavior, i.e. the increase in apparent extensional viscosity with apparent strain rate, occurs at least one decade in strain rate after the onset of shear-thinning behavior. Raising the concentration made the apparent extensional viscosity higher, and lowered the apparent extension rate at which thickening was first observed. This trend, but not the actual viscosity values, correlates well with the extensional viscosity measurements on another series of PEO solutions with a fiber-spinning device by Hudson et al. (1988). The shape of the apparent extensional viscosity versus apparent extension rate curves is also remarkably similar to that of semidilute solutions of wormlike micelles reported by Hu et al. (1994) and by Walker et al. (1996). Wormlike micelles are thought to behave as ideal monodisperse polymer solutions.

An important comparison can be made between the apparent extensional viscosity of Newtonian liquid D and 0.38% PEO solution. The low shear viscosity of the polymer solution is approximately 13 mPa s and that of liquid D is 11 mPa s. They also show similar behavior in extension albeit the extensional viscosity of the PEO solution starts rising at a lower extension rate, about 100 s^{-1}. While the thickening behavior of the PEO solution may reflect actual material properties, that of Newtonian liquid D is due to fluid mechanical effects in the instrument.

The sharp drop in apparent extensional viscosity at high rates, e.g. beyond apparent strain rate of 2000 s^{-1} with the 0.95% PEO solution, is believed to be an instrument artifact, because the torque never attained steady values during the experiment. The ratio of the low-rate apparent extensional viscosity to the zero-shear viscosity *varies with concentration*. This ratio is $T_A \approx 5$ for the 0.95 wt.% PEO solution, and it is $T_A \approx 3$ for the 1.26 wt.% PEO solution. Torques registered with the other less concentrated solutions were below the minimum specifications for the transducer, and hence their apparent extensional viscosities could not be measured.

Conclusions

This paper evaluates measurements of uniaxial extensional viscosity with opposed-nozzle devices. The presence of both shear and extensional kinematics in most of the flow and the inability to generate a true extensional flow field except in the immediate neighborhood of the stagnation point (Winter et al., 1979) cause the measured viscosity to differ from the true material property. Moreover, not only extensional stresses, but also dynamic pressure, shear stresses and momentum of the liquid all contribute to the measured force (Schunk et al., 1990; Pasquali and Scriven, 1996). In view of these, opposed-nozzle devices can at best be used as indexers.

Apparent extensional viscosities of Newtonian liquids over a wide range of shear viscosities were measured with a commercial opposed-nozzle device. The shear viscosities of the liquids tested varied from 1 to about 800 mPa s. Nozzles of different diameter were used and measurements taken at the same extension rate with different nozzles agreed within less than 10%. Each nozzle pair was used to measure extensional viscosity over about one to two orders of magnitude in apparent extension rate. Reynolds numbers ($\mathrm{Re} \equiv \frac{\rho Q \bar{h}}{\eta_S \pi R^2}$) were approximately unity at the higher limit of each

range except for the lowest viscosity liquids. Most of the measurements were made with nozzles of diameter 1–5 mm, except for the lowest viscosity liquids. The flow between the smallest nozzles (0.5 mm in diameter) was found to be extremely sensitive to nozzle alignment, and hence these nozzles were used only to reproduce the observations of Hermansky and Boger (1995). Measurements were taken only when the torque reached a steady value indicated on a chart recorder.

The ratio of the apparent extensional viscosity to the shear viscosity $T_A \equiv \eta_E/\eta_S$, some times inappropriately called Trouton ratio, of even Newtonian liquids was found to be greater than 3, confirming the calculations of Schunk et al. (1990). This ratio was found to vary from 4.5 to 7 for the Newtonian liquids A, B, C used in this study.

Apparent extensional viscosity of Newtonian liquids falls slightly at $\mathrm{Re} \approx 1$ and then rises sharply with strain rate. Inertia *lowers* the torque, and hence the apparent extensional viscosity measured with opposed-nozzles devices, contrary to the suggestion of Anklam et al. (1994) and Hermansky and Boger (1995). One of the reasons for the rise at higher rates could be a lower dynamic pressure at the stagnation plane, due to increased viscous dissipation in the whole flowing liquid in the beaker. Hermansky and Boger's correction was examined and found to over-correct measurements by a factor of 100. Moreover, the basis for their correction is purely empirical and unrelated to liquid inertia. The flow was also analyzed by computer-aided solution of the Navier-Stokes equation system. The calculated inertia contribution is about 30% of that predicted on the basis of uniaxial extension in $0.1 \leq \mathrm{Re} \leq 10$. However, in the light of the observations with Newtonian liquids, corrections based on Newtonian liquids to the apparent extensional viscosities of non-Newtonian liquids are not recommended.

The effect of the ratio of nozzle separation to diameter on the average residence time of the liquid was analyzed by assuming uniaxial extensional flow, i.e. $\boldsymbol{v} = \dot{\varepsilon} z \boldsymbol{e}_z - \dot{\varepsilon} \frac{r}{2} \boldsymbol{e}_r$. The residence time of the liquid averaged over the nozzle face is independent of this ratio, provided the region of radial inflow does not depend on nozzle separation, but there is no theoretical reason that it should. Experiments show that in some cases the wider the gap, the lower the extensional viscosity, whereas in other cases the opposite is true. More visual information on the flow field is needed to relate the average residence time of the liquid to nozzle separation.

The observations suggest that opposed-nozzle devices can be used to quantify the extensional behavior of liquids at Reynolds numbers less than unity. At higher Reynolds numbers, several other effects may become important. The delicate balance of dynamic pressure, shear in the flow and on the nozzle walls, and liquid inertia is altered and the measured viscosity rises. Apparent extensional viscosities of liquids whose shear viscosities are less than about 50 mPa s cannot be reliably measured with the Rheometrics RFX due to a combination of transducer sensitivity and high Reynolds number effects.

The use of opposed-nozzle devices to index low viscosity polymer solutions was demonstrated with a series of solutions of high molecular weight poly(ethylene oxide) in water. The key to obtaining reproducible measurements on elastic liquids proved to be choosing a delay time long enough that the torque can reach a steady value. Measurements with the same nozzle pairs were reproducible from run to run, and measurements obtained with different diameter nozzles at the same extension rate agreed to within less than 10%. Opposed-nozzle devices can be used to index dilute polymer solutions at higher Reynolds numbers (see Hermansky and Boger, 1995), but in that regime the flow may lose part of its extensional character, and the relative contribution of extensional stresses to the torque measurements may decrease. The measurements then will not reflect actual liquid behavior in extensional flows, but rather a combination of extensional response and several other effects.

Acknowledgments The authors are grateful to Dr. Mahesh Padmanabhan and Dr. David W. Giles for many insightful discussions on the intricacies of opposed-nozzle devices. This work was supported by industrial and National Science Foundation funds through the Center for Interfacial Engineering at the University of Minnesota.

Appendix A

Hermansky and Boger's (1995) inertia correction

Hermansky and Boger (1995) proposed that inertia of the liquid entering the nozzles raises the measured torque at high strain rates. Their correction to the viscosity of Newtonian liquids is reproduced here (Eq. (7) in their paper):

$$\eta_{\mathrm{corrected}} = \eta_{\mathrm{apparent}} - \frac{a'(R)\rho d^2}{4\pi L R^2}\dot{\varepsilon} \tag{20}$$

where $\eta_{\mathrm{corrected}}$ is the corrected viscosity, η_{apparent} is the measured viscosity, $a'(R)$ is a constant that depends only on nozzle size, ρ is the density of the liquid, d is *half* the distance between nozzles, $L(=7.62\ \mathrm{cm})$ is the length of the nozzle arm, and R is the radius of the nozzle. Hermansky and Boger estimated $a'(R)$ to be 0.708, 2.64 and 16.8 cm^3 for nozzles of diameter 0.5, 1.0 and 2.0 mm respectively (p. 9 of their paper).

The results of this correction applied to the measured apparent extensional viscosity of liquids C–E are shown in Fig. A1. The correction calculated from Eq. (20) is

Rheologica Acta, Vol. 36, No. 4 (1997)

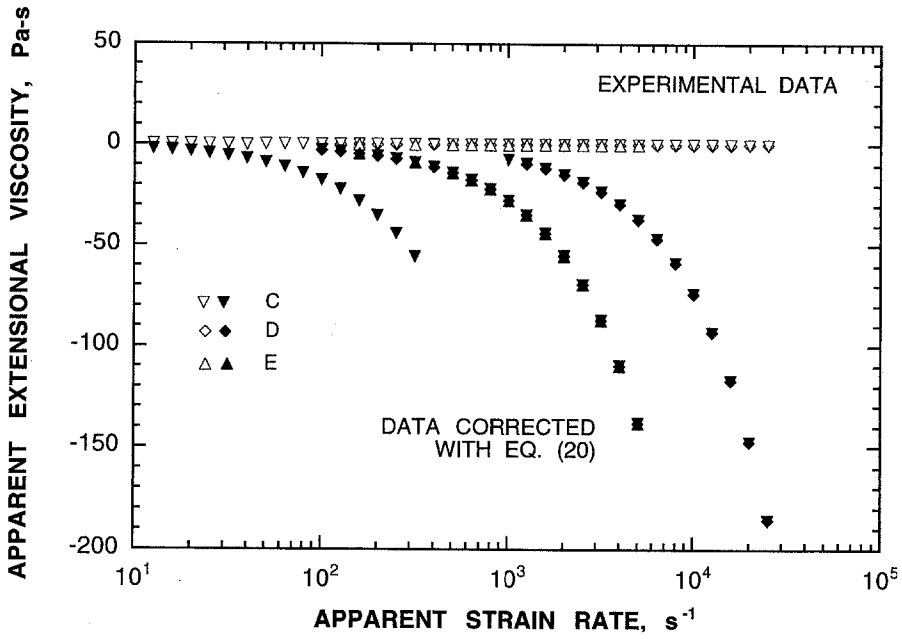

Fig. A 1 Comparison of apparent extensional viscosity and the corrected extensional viscosity of liquids C–E after applying Eq. (20) (Hermansky and Boger 1995) and using density $\rho = 1000\ kg/m^3$. Open symbols are the measured apparent extensional viscosity, while the solid symbols represent the corrected viscosity. The correction results in large negative values of the viscosity which is aphysical

Table A 1 Comparisons between corrections proposed in Eq. (24) by Hermansky and Boger (1995) and Eq. (25). Data from Fig. 3 of their paper

η_S [Pa s]	$\dot{\varepsilon}$ [s^{-1}]	$\eta_{apparent}$ [Pa s]	$\eta_{corrected}$ Eq. (20) [Pa s]	$\eta_{corrected}$ Eq. (25) [Pa s]	$\eta_{corrected}/\eta_S$ Reported	$\eta_{corrected}/\eta_S$ Eq. (25)
0.001	5000	0.03	–3.67	–0.007	30	–7
0.001	20000	0.15	–14.64	0.002	150	2
0.0036	5000	0.054	–3.64	0.017	15	4.7
0.0036	20000	0.198	–14.59	0.050	55	13.9
0.0055	5000	0.055	–3.64	0.018	10	3.3
0.0055	20000	0.165	–14.62	0.017	30	3.3
0.077	5000	0.385	–3.31	0.348	5	4.5

too large, and the corrected viscosities are large and negative. Table A 1 shows the same correction applied to the data in Fig. 3 of Hermansky and Boger's paper, and the same trend is observed.

The reasons for this discrepancy are explained below. Hermansky and Boger used the following equations to calculate the measured viscosity, average strain rate, and velocity U of the liquid entering the nozzle (Eqs. (1, 3 and 4) in their paper, respectively):

$$\eta_{apparent} = \frac{Md}{2QL} \tag{21}$$

$$\dot{\varepsilon} = \frac{2Q}{\pi R^2 d} \tag{22}$$

$$U = \dot{\varepsilon}\frac{d}{2} \tag{23}$$

where Q is the flowrate into one nozzle. The above equations are inconsistent with their definition of d as half the distance between the nozzles. In fact, d is the *total* distance between the nozzles, $d = 2h$ (cf. Eqs. (1 and 2)). This error is propagated until their inertia correction reads (Eq. (8))

$$\frac{\eta_{corrected}}{\eta_S} = \frac{\eta_{apparent}}{\eta_S} - \frac{a'(R)\rho d^2}{4\pi L R^2 \eta_S}\dot{\varepsilon} \tag{24}$$

where η_S is the shear viscosity, and $\eta_{corrected}/\eta_S$ was inappropriately (for reasons described in the introduction of this article and in Schunk et al., 1990) forced to 3.

Further, Hermansky and Boger assumed that the liquid density ρ was $1000\ kg/m^3$ in plotting the prefactor $a'(R)\rho d^2/4\pi L R^2 \eta_S$ against $1/\eta_S$ (Fig. 8 in their paper). The apparent linear relationship between the two quantities then allowed them to estimate $a'(R)$ from the slope of the line and knowledge of the nozzle size, separation and L. However the viscosity units employed (cP) did not agree with the c.g.s. system used. Hence, $a'(R)$ was overestimated by a factor 100.

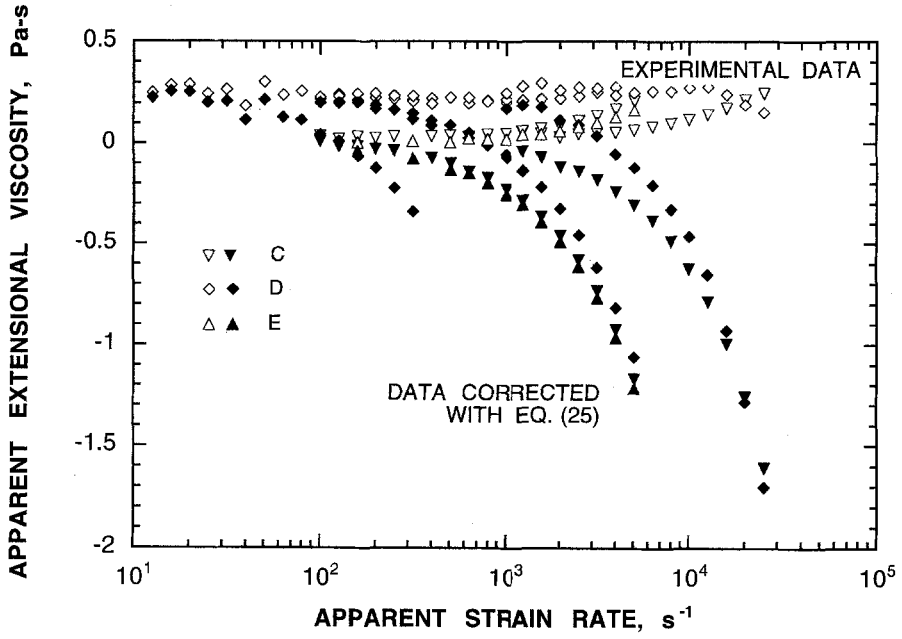

Fig. A 2 Comparison of apparent extensional viscosity and the corrected extensional viscosity of liquids C–E on application of Eq. (25). Open symbols are the measured apparent extensional viscosity, while the solid symbols represent the corrected viscosity. This correction also results in negative values of the viscosity at high strain rates, though not as large as those predicted in Fig. A 1 by Eq. (20)

Equation (24) can be correctly reformulated by using appropriate units and a consistent definition of nozzle separation, but still considering density constant. The corrected version of Eq. (24) under the assumption of constant density is

$$\frac{\eta_{\text{corrected}}}{\eta_S} = \frac{\eta_{\text{apparent}}}{\eta_S} - \frac{a^*(R)\rho h^2}{\pi L R^2 \eta_S}\dot{\varepsilon} \tag{25}$$

where $a^*(R) = a'(R)/400$. Table A 1 and Fig. A 2 respectively show how this correction applies to Hermansky and Boger's data on low viscosity Newtonian solutions and to liquids, C, D and E defined in Table 2.

A better reformulation of this "inertia correction" (Eq. (25)) is

$$\frac{\eta_{\text{corrected}}}{\eta_S} = \frac{\eta_{\text{apparent}}}{\eta_S} - A\left(\text{Re}, \frac{h}{R}\right)\frac{\rho h^2 \dot{\varepsilon}}{\eta_S} = \frac{\eta_{\text{apparent}}}{\eta_S} - A\left(\text{Re}, \frac{h}{R}\right)\text{Re} \tag{26}$$

where $A(\text{Re}, \frac{h}{R})$ is a *dimensionless* factor. By using the data reported by Hermansky and Boger, the value of $A(R)$ is found to be 0.118, 0.110 and 0.176 for nozzles of diameter $2R$ equal to 0.5, 1 and 2 mm respectively.

The use of Eq. (26) to correct data *is not recommended.* The reason is that Eq. (26) is completely empirical. Its applicability and limitations can not be predicted because it is not based on any momentum balance (see section on "Effect of high flow rates").

References

Aken JA van, Janeschitz-Kriegl H (1980) New apparatus for the simultaneous measurement of stresses and flow birefringence in biaxial extension of polymer melts. Rheol Acta 19:744–752

Anklam MR, Warr GG, Prud'homme RK (1994) The use of opposed nozzles configuration in the measurements of extensional rheological properties of emulsions. J Rheol 38:797–810

Cai JJ, Souza Mendes PR, Macosko CW, Scriven LE, Secor RB (1992) A comparison of extensional rheometers. In: Moldenaers P, Keunigs R (eds) Theoretical and applied rheology. Proc. XIth Intl. Congr. on Rheology, Brussels, Belgium, 1012

Cathey CA, Fuller GG (1988) Uniaxial and biaxial extensional viscosity measurements of dilute and semi-dilute solution of rigid rod polymers. J Non-Newt Fluid Mech 30:303–316

Cathey CA, Fuller GG (1990) The optical and mechanical response of flexible polymer solutions to extensional flow. J Non-Newt Fluid Mech 34:63–88

Chow A, Keller A, Müller AJ, Odell JA (1988) Entanglements in polymer solutions under elongational flow: a combined study of chain stretching, flow velocimetry, and elongational viscosity. Macromolecules 21:250–256

Clark RC (1991) Extensional viscosity of some food hydrocolloids. Presented at Sixth International Conference on Gums and Stabilizers for the Food Industry, Wrexham, Wales, July 15–19

Frank FC, Keller A, Mackley MR (1971) Polymer chain extension produced by impinging jets and its effect on polyethylene solution. Polymer 12:467–473

Fuller GG, Cathey CA, Hubbard B, Zebrowski BE (1987) Extensional viscosity measurements for low-viscosity fluids. J Rheol 31:235–249

Hermansky CG, Boger DV (1995) Opposing-jet viscometry of fluids with viscosity approaching that of water. J Non-Newt Fluid Mech 56:1–14

Hu Y, Wang SQ, Jamieson AM (1994) Elongational flow behavior of cetyltrimethylammonium bromide/sodium salicylate surfactant solutions. J Phys Chem 98: 8555–8559

Hudson NE, Ferguson J, Warren BCH (1990) Polymer complexation effects in extensional flows. J Non-Newt Fluid Mech 34:63–88

Keller A, Müller AJ, Odell JA (1987) Entanglements in semi-dilute solutions as revealed by elongational flow studies. Polymer and Colloid Sci 75:179–200

Laun HM, Hingmann R (1990) Rheological characterization of the fluid M1 and of its components. J Non-Newt Fluid Mech 35:137–157

Mackay ME, Dajan AM, Wippel H, Janeschitz-Kriegl H, Lipp M (1995) An approximate technique to determine elongation stresses in stagnation flow. J Rheol 39:1–14

Mackley MR, Keller A (1975) Flow induced polymer chain extension and its relation to fibrous crystallization. Phil Trans Roy Soc London A 278:29–66

Macosko CW (1994) Rheology: principles, measurements and applications. VCH, New York

Macosko CW, Ocansey MA, Winter HH (1982) Steady planar extension with lubricated dies. J Non-Newt Fluid Mech 11:301–316

Mikkelsen KJ, Macosko CW, Fuller GG (1988) Opposed jets: an extensional rheometer for low viscosity liquids. In: Uhlherr PHT (ed) Proc. Xth Intl. Congr. on Rheology, Sydney, Australia, vol 2, 125–127

Newman AA (1968) Glycerol. Morgan-Grampion, London

Nekton 3.0 User's Guide (1995) Fluent Inc., Lebanon NH

Padmanabhan M (1995) Measurement of extensional viscosity of viscoelastic liquid foods. J Food Eng 25:311–327

Pasquali M, Scriven LE (1996) Extensional flows and extensional rheometry. In: Aït-Kadi A, Dealy JM, James DF, Williams MC (eds) Proc. XIIth Intl. Congr. on Rheology, Québec City, Canada, 727–728

Pope DP, Keller A (1977) A study of the chain extending effect of elongational flow in polymer solutions. Colloid and Polymer Sci 256:751–756

Rheometrics Fluid Analyzer RFX Owner's Manual (1991) Rheometrics, Inc., Piscataway, NJ

Schunk PR, de Santos JM, Scriven LE (1990) Flow of Newtonian liquids in opposed-nozzles configuration. J Rheol 34:387–414

Schunk PR, Scriven LE (1990) Constitutive equation for modeling mixed extension and shear in polymer solution processing. J Rheol 34:1085–1119

Schweizer T, Mikkelsen K, Cathey CC, Fuller GG (1990) Mechanical and optical response of the M1 fluid subject to stagnation point flow. J Non-Newt Fluid Mech 35:277–286

Secor RB, Schunk PR, Hunter TB, Stitt TF, Macosko CW, Scriven LE (1989) Experimental uncertainties in extensional rheometry of liquids by fiber drawing. J Rheol 33:1329–1358

Taylor GI (1934) The formation of emulsions in definable fields of flow. Proc R Soc A 146:501–523

Walker LM, Moldenaers P, Berret J-F (1996) The macroscopic response of wormlike micelles to elongational flow. Langmuir (accepted for publication)

Willenbacher N, Hingmann R (1994) Shear and elongational flow properties of fluid S1 from rotational, capillary, and opposed jet rheometry. J Non-Newt Fluid Mech 52:163–176

Winter HH, Macosko CW, Bennett KE (1979) Orthogonal stagnation flow, a framework for steady extensional flow experiments. Rheol Acta 18:323–334